New Frontiers in Modern Resonator Spectroscopy

Maksim A. Koshelev, Igor I. Leonov, Evgeny A. Serov, Alena I. Chernova, Aleksandr A. Balashov, Grigoriy M. Bubnov, *Member, IEEE*, Aleksandr F. Andriyanov, Aleksandr P. Shkaev, Vladimir V. Parshin, Andrei F. Krupnov, and Mikhail Yu. Tretyakov

***Abstract*—New opportunities due to the advancements in the techniques and methods of broadband resonator spectroscopy in the millimeter and submillimeter range (also known as the terahertz region) are considered in this paper. An upgraded variant of the spectrometer produced at the Institute of Applied Physics, Russian Academy of Sciences (Nizhny Novgorod, Russia) possessing a sensitivity to the absorption coefficient of approximately 4×10^{-9} cm^{-1} is presented. The spectrometer allows the continuous recording of gas spectra in the 45–500 GHz frequency range (six waveguide subbands) at pressures of 10–1000 torr. A fully automated spectrum recording within the waveguide subband reduces the overall time required for the experiment by almost an order of magnitude. Examples of recording the spectra of oxygen and water vapor resonance lines, as well as of continuum absorption, including the rotationally resolved water dimer spectrum, are presented. It is demonstrated that the uncertainty of measuring the broadening parameter of diagnostic atmospheric lines may be reduced to 0.1%, which meets the stringent present-day requirements of remote sensing of the atmosphere. The physically attainable ultimate sensitivity of broadband microwave resonator spectrometers of various types is discussed. Prospects for further development of the spectrometer and its application for solving fundamental and applied problems of spectroscopy are analyzed.**

***Index Terms*—Broadband resonator spectroscopy, millimeter (mm) and submillimeter (submm) wave measurements, high-precision spectroscopy.**

I. Introduction

RESONATOR spectroscopy of gases has a long history. A box (sometimes the size of a room) with polished copper walls played the role of the resonator in the first spectrometers. The problem of a large number of modes being excited in such a volumetric resonator was solved by means of a fan that intermixed the radiation inside the box and a large number of thermocouples that measured the temperature of the gas heated by the radiation (see, for example, [1]). As stated in the classical spectroscopy book by Townes and Schawlow [2], the use of a resonator allows absorption measurements in broad lines and large interaction lengths to be attained in gas cells of small size. A few years later, in the paper [3] devoted to the theory of resonator spectrometers, it was shown that, other things being equal, the ultimate sensitivity can be up to 300 times higher than that of a video spectrometer with a conventional 3-m cell. Beers' paper appeared at the time the culture of working with open resonators with two reflecting surfaces (Fabry–Perot resonators) had formed. This stimulated the creation of resonator spectrometers in the 1960s, considered at that time as an alternative to video spectrometers, which would provide a higher sensitivity while maintaining the high resolution inherent to microwave spectroscopy. The high sensitivity of resonator spectrometers is due to multiple passages of radiation through the studied gas as a result of repeated reflections from the mirrors in the Fabry–Perot resonator. In a high-Q resonator, the effective path length can be on the order of 1 km, which is practically impossible in ordinary gas cells in the millimeter (mm) and submillimeter (submm) ranges, in which narrow nondivergent beams cannot be formed.

A typical example of a pioneering work on microwave resonator spectroscopy is the creation of a resonator spectrometer by Valkenburg and Derr [4], which was used for studying high-resolution spectra of D_2O [5] and N_2O [6] molecules in the 70–310 GHz range. It was shown that, owing to technical features, the real sensitivity of the resonator spectrometers was no higher than that of conventional video spectrometers. The main reason for this (the complexity of employing modulation methods) was mentioned in [3] but was apparently undervalued by other researchers.

Despite the failure to achieve record sensitivity in investigations of high-resolution spectra, resonator spectrometers demonstrated advantages in precise measurements of absorption coefficients [7], [8], as well as in the study of broad atmospheric lines [9] and nonresonant absorption [10].

The next impetus for the further advancement of resonator spectroscopy was given by radar and remote sensing systems, which required accurate models for the propagation of mm and submm radiations in the atmosphere, whereas the information provided by the high-resolution molecular spectroscopy was incomplete. Typical examples of instruments intended to solve these problems are the spectrometers developed at the Institute

Manuscript received May 18, 2018; revised July 22, 2018; accepted September 27, 2018. Date of publication October 11, 2018; date of current version December 11, 2018. The spectrometer software and hardware upgrade were supported by the Russian Foundation for Basic Research Grants No. 18-02-00705 and 18-05-00698, respectively. The experimental study of water vapor spectrum was supported by Russian State Project no. 0035-2014-0034. *(Corresponding author: Evgeny A. Serov.)*

M. A. Koshelev, I. I. Leonov, E. A. Serov, A. I. Chernova, G. M. Bubnov, A. F. Andriyanov, A. P. Shkaev, V. V. Parshin, A. F. Krupnov, and M. Yu. Tretyakov are with the Institute of Applied Physics, Russian Academy of Sciences, Nizhny Novgorod 603950, Russia (e-mail: koma@ipfran.ru; leonov@ipfran.ru; serov@ipfran.ru; alena_chernova@ipfran.ru; bubnov@ieee.org; andriyanov@ipfran.ru; shkaevap@mail.ru; parsh@ipfran.ru; kru@ipfran.ru; trt@ipfran.ru).

A. A. Balashov is with the Lobachevsky State University of Nizhny Novgorod, Nizhny Novgorod 603950, Russia (e-mail: abab-2012@yandex.ru).

Color versions of one or more of the figures in this paper are available online at http://ieeexplore.ieee.org.

Digital Object Identifier 10.1109/TTHZ.2018.2875450

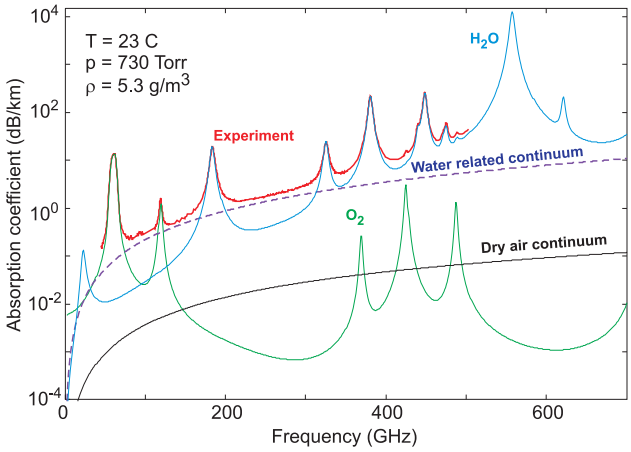

Fig. 1. Broadband experimental recording of the atmospheric air spectrum and the calculated contribution of its four different components: H_2O resonance spectrum, O_2 resonance spectrum, dry air continuum, and water-related continuum.

for Telecommunication Science (Boulder, CO, USA), by Liebe *et al.* [11]–[13] and at Lille University (Lille, France) [14].

The development of modern resonator spectroscopy is stimulated by the growing demands for the accuracy of radiation propagation models, as well as the desire to find a modulation method that would be efficient for a resonator spectrometer and make use of its potential advantage in sensitivity. One possible approach relies on pulsed excitation of the resonator and recording its response in the time domain in a very short time specified by the resonator time constant. This method is widely known as cavity ringdown spectroscopy (CRDS). An attempt to implement this approach was made in the spectrometer of Ohio State University (USA) [15]. This approach has been fully realized with a record sensitivity to the radiation absorption coefficient of up to 1.4×10^{-13} cm^{-1}, so far only in resonator spectrometers in the infrared (IR) range (see, for example, [16]–[19]), where the reflection losses from mirrors can be two orders of magnitude smaller than the minimum achievable losses in the mm and submm ranges, which, other things being equal, provides a much higher Q-factor of the resonator.

Another resonator spectroscopy approach is the fast, repetitive recording of the resonant response shape in the frequency domain during the same extremely short time period. Special high-precision frequency modulation of radiation is used for recording. This approach is currently possible in our spectrometer, and its unique capabilities are detailed in the work [20]. Since then, several versions of the spectrometer have been developed aimed at maximum implementation of its potential and allowing the widest possible range of conditions (frequency range, pressure, temperature, etc.) at which measurements can be made. These stages can be traced in [21]–[24].

The progress made in the technical development of the spectrometer and the improvement of the methods for registering spectra enabled high-precision studies of the oxygen band profile near 60 GHz, as well as of major atmospheric diagnostic lines of water vapor and oxygen in a range of up to 500 GHz [25]. An example of a broadband recording of the atmospheric air spectrum is shown in Fig. 1. Moreover, the resonator spectrometer permitted, for the first time, the detection and investigation of the rotationally resolved spectrum of the water dimer in water vapor at room temperature [26], [27].

In the recent version of The Ohio State University spectrometer described in [28], the resonator response recording is transferred from the time to the frequency domain, but the currently attained sensitivity is 4×10^{-7} cm^{-1}, which does not exceed the result of the work [15]. In paper [22], a sensitivity of 9×10^{-9} cm^{-1} was demonstrated in the recording of the oxygen line near 118 GHz, consistent with a double variation sensitivity of 4×10^{-9} cm^{-1} from the basic paper [20], which was also cited by Nagarajan *et al.* [28].

In this paper, we review the state-of-the-art capabilities of the spectrometer and discuss prospects for its further development and applications. The principles of operation of the spectrometer, its design, and the upgraded elements are addressed in Section II. Section III concerns the method for retrieving the spectrum of the studied gas from primary experimental data. Examples of studies demonstrating the measurement accuracy of parameters of the most important diagnostic atmospheric lines are presented in Section IV. The physically attainable ultimate sensitivity of wide-range microwave resonator spectrometers of various types is analyzed in Section V. Prospects for further development of the spectrometer and increasing its sensitivity up to the maximum achievable level are discussed in Section VI.

II. New Version of the Resonator Spectrometer

The spectrometer block diagram is presented in Fig. 2. The general scheme of the spectrometer is similar to that in the previous version described in detail in [22] and [23]. The studied gas is inside a high-Q ($Q = f/\Delta f \approx 10^6$) Fabry–Perot resonator excited by continuous wave coherent radiation of a backward wave oscillator (BWO). The radiation frequency is controlled by a phase-locked-loop (PLL) system that allows the excitation of the resonator by fast step-by-step frequency scanning of the radiation without phase jumps during switching, which is ensured by the use of a direct digital synthesizer (DDS). Absorption in the gas is determined at the frequencies of successive eigen modes of the resonator via changes in its Q-factor determined by radiation energy losses in the resonator when a sample is placed into it. The absorption coefficient α in the small optical depth approximation ($\alpha L \ll 1$, where L is the resonator length) is defined by

$$\alpha = 2\pi(\Delta f - \Delta f_0)/c \tag{1}$$

where c is the speed of light in the gas under consideration and Δf and Δf_0 are the resonance curve widths measured when the resonator is filled with the studied gas and with nonabsorbing gas, respectively. The nonabsorbing gas provides a constant optical path length in the resonator in both series of measurements. We generally use argon, with the pressure chosen such that its refraction index should be equal to that of the studied gas. It is important that the intrinsic losses of the resonator and the losses of the resonator filled with the studied gas are measured strictly at the same frequencies.

The condition of small optical depth is not a principal limitation of the spectrometer. It may also be used for investigating

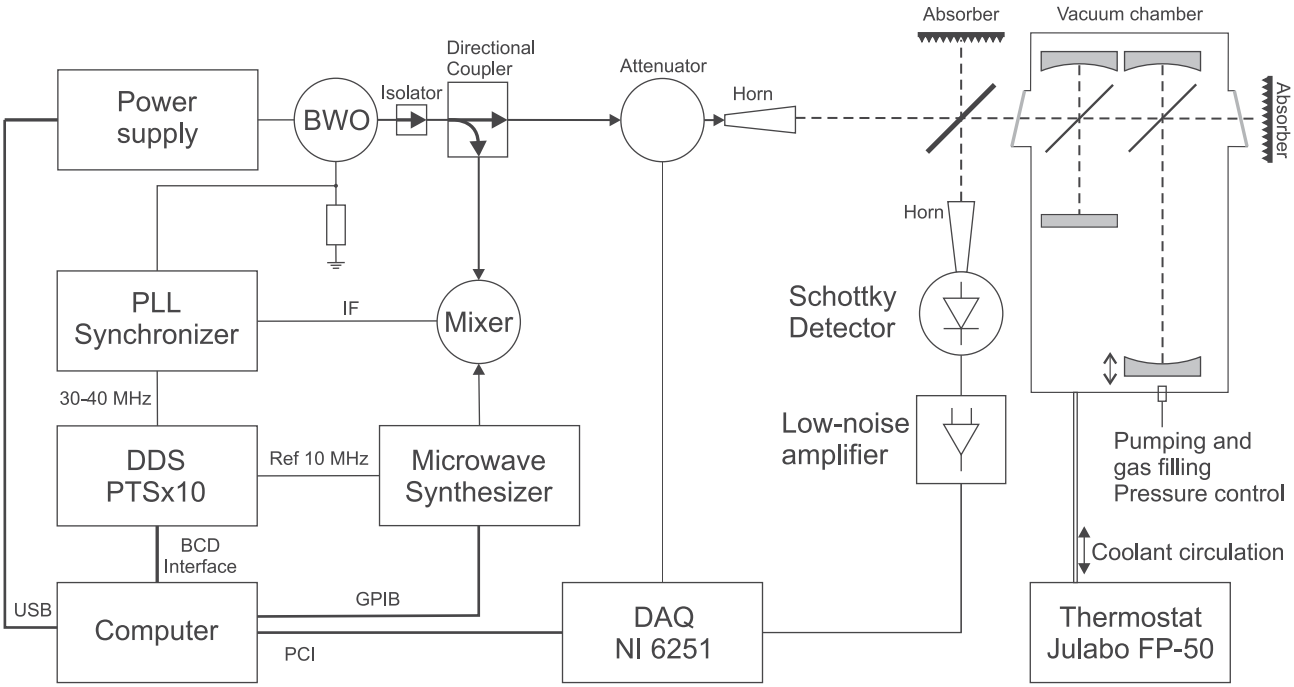

Fig. 2. Spectrometer block diagram.

strongly absorbing gases if a more exact formula is used instead of (1) [29].

The spectrometer sensitivity corresponding to the minimum detectable absorption coefficient of the gas is directly related to the accuracy of measuring the resonance curve width. Therefore, the main improvements in the spectrometer were aimed at increasing this accuracy.

One of the influencing factors is the temporal stability of the resonator parameters (length, intrinsic losses, and parameters of the studied gas) and the dimensions of the waveguide line, including its quasioptical part. Note that the long-term stability of the radiation power is not essential because the measured value is the width of the resonance curve, which does not depend on the response amplitude. The variability of the influencing parameters leads to an uncontrolled systematic error in determining α using formula (1). Natural ways to reduce this error are: 1) increasing the system stability and 2) increasing the spectrum recording speed. The new version of the spectrometer is improved in both respects.

To ensure the temperature and pressure stability, the Fabry–Perot resonator is placed in a stainless steel vacuum chamber with a volume of approximately 200 L coated on the outside with foam polyethylene for thermal insulation from the environment. The temperature is stabilized at a preset level by means of a Julabo FP-50 thermostat, which can set the coolant temperature at the output to an accuracy of 0.01 °C. The coolant circulates over a copper tube attached to a thick-wall (5 mm) copper casing with the resonator inside.

If needed, a "cold finger" technique may be used during the experiment to maintain a stable humidity for the studied gas. This technique is based on maintaining a stable temperature of the flask with water, which is permanently connected to the chamber. As the pressure of saturated water vapor is temperature dependent, a water vapor pressure equal to the saturated vapor pressure in the flask is established in the whole system. The temperature of the flask is also stabilized by the Julabo FP-50 thermostat. As a result, a stability of the water vapor pressure of 0.01 torr at a pressure of approximately 10 torr is attained inside the chamber at room temperature.

It is important to maintain a constant temperature for the elements of the entire waveguide line because parasitic reflections in the line interfere with useful signals, which lead to modulation of the measured values of Δf and Δf_0, with the phase depending on the length of the waveguide line (for more details, see Section III). If the length of the line is fixed, the modulation effect is subtracted and does not affect the resulting spectrum. For this, we stabilize the air temperature in the room by an air conditioner and the waveguide line by a thermostat. As a result, a temperature stability of ± 0.2 °C is reached in the waveguide line. The faster the spectrum is recorded, the easier it is to ensure stable conditions.

In the new version of the spectrometer, a commercial DDS synthesizer PTS-10 (Programmed Test Sources, Inc.) controlled via a fast synchronous BCD parallel interface is used. The upgraded system, which automatically records the spectra, reduces the recording time by approximately an order of magnitude in comparison with the previous version of the spectrometer [22]. The computer automatically controls the BWO power supply voltage, the frequency and power of the microwave synthesizer, and the position of the attenuator to ensure the constant amplitude of the resonance response curve. It also monitors the state of the PLL system, scans the DDS frequency step by step, synchronously reads the detector data on the amplitude of the resonator response from the analog-to-digital converter, and processes the data to determine the width of the resonance curve.

Spectrum recording includes two series of measurements. First, the "baseline" is recorded, i.e., the values of Δf_0 at the frequencies of successive longitudinal modes of a fixed-length resonator filled with nonabsorbing gas. This recording determines the intrinsic losses of the resonator, including diffraction, coupling, and reflection losses. Second, the Δf values of the resonator filled with the gas under study are recorded at the same frequencies.

Before the recording is started, the list of mode frequencies is calculated and loaded into the computer. The resonator spectrum is very close to an equidistant one, with free spectral range (FSR) $\Delta F = c/2L$. With a resonator length of approximately 40 cm, the distance between the modes is approximately 360 MHz. With such a nontunable resonator, the spectrum will be recorded point by point at every 360 MHz. This discreteness is acceptable for studying atmospheric lines with half-widths of 3–10 GHz. In the case of narrower lines, several spectra are recorded at different lengths of the resonator, which is implemented by the stepwise movement of one of the mirrors. This provides the required number of points on the studied molecular line at any gas pressure. Of course, the baseline is recorded for each space between the mirrors.

The frequency of the microwave synthesizer and the voltage of the BWO power supply unit are preset so that the frequency of the BWO radiation locked by the PLL is close to the frequency of the first resonator mode in the considered spectral range. A preliminary scan of the radiation is made by the DDS near this frequency. The detected signal is digitized and processed by the computer. If the resonator response in the desired mode is within the scan area, the software adjusts the center frequency, the width of the scanning range, and the attenuator position. After that, repeated "working" scanning of the radiation frequency in a narrow frequency interval is performed. The response profile is recorded and then approximated by a model function based on the Lorentz profile for determining the resonance width averaged over all recordings. Scanning is performed "back and forth" a desired number of times. The statistical error of the absorption coefficient measurements as a function of the number of scans is illustrated in Fig. 3. The presented curves were obtained as a result of analyzing 300 000 scans at a fixed frequency near 105 GHz, from which it follows that, in this spectrometer, the optimal number of scans is 100–150. After that, the statistical error in determining the resonance width begins to deviate from the $N^{-0.5}$ law. The corresponding variational sensitivity of the absorption coefficient amounts to $\sim 1.5 \times 10^{-9}$ cm^{-1}.

The center frequency, width, and amplitude of the resonance profile are determined immediately after recording by optimizing the parameters using the following model function:

$$L\_\mathrm{mod}(f) = A \cdot \frac{1 + a_1 \cdot (f - f_0)}{1 + \left(\frac{f - f_0}{\Delta f}\right)^2} + b_0 + b_1 \cdot (f - f_0) \quad (2)$$

where f_0 is the central frequency, Δf is the half-width at half-maximum, A is the amplitude, and a_1, b_0, and b_1 are variable parameters taking into account the distortion of the profile due to parasitic reflections in the waveguides and imperfect zero setting of the amplifiers.

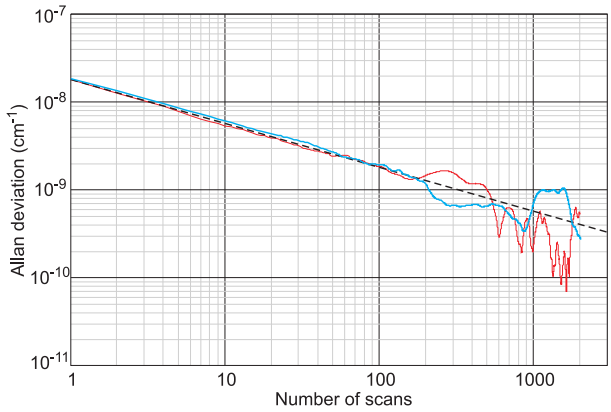

Fig. 3. Allan variance plot for $2\pi\Delta f/c$ (1) versus number of triangle scans. The red and blue curves were obtained from two independent experimental trials. The dashed line is the $N^{-0.5}$ dependence. The duration of each scan was 52 ms.

As soon as the working scan is completed, the BWO frequency is automatically switched to the next resonator mode, and the process is repeated for the entire mode list. The PLL regime of the BWO frequency is maintained throughout the recording.

Obviously, the more the number of scans made per unit time, the faster the spectrum is recorded for a given number of averages of the measured response width. Therefore, the time between the switching of the DDS frequency τ_f is one of the most important parameters of the spectrometer. The characteristic time constant of the resonator τ_{res} is 1–2 μs. In the present version of the spectrometer, τ_f can be reduced to 2–3 μs. However, as τ_f decreases to a value of the order of τ_{res}, the resonator response will deviate from the Lorentz profile. In this situation, the use of model (2) will lead to a systematic overestimation of the response width. This problem may be solved by using a more adequate model [30]. With the use of this model, the time required for computer processing of the response recording is increased when the scanning speed is accelerated. This is not a fundamental limitation, but in practice, it leads to a reduction in the spectrum recording speed, indicating the need to optimize the speed of the DDS frequency scanning.

The bandwidth of the radiation receiver is another factor that needs to be taken into account when the scanning speed is increased. Narrowing of the receiver band is an analog method of signal accumulation averaging the noise. If the time required for a single frequency scan is shorter than the time required for characteristic mechanical or electrical noise distorting the response profile, then both of these noise reduction mechanisms (averaging the measured response width at multiple scanning and determining the width of response recorded by the narrowband receiver at slow scanning speed) are equivalent, and the application of either does not restrict the ultimate sensitivity of the spectrometer.

The time required for recording the spectrum is not proportional to τ_f. For each resonator mode, in addition to

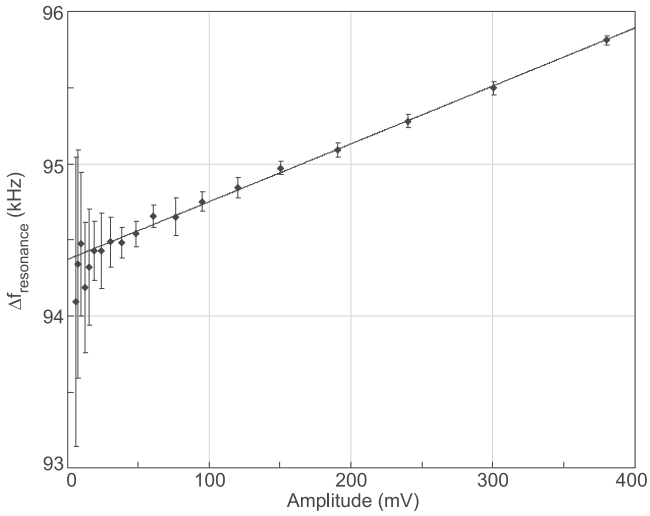

Fig. 4. Resonance curve half-width obtained from the fit (averaged over 128 scans) versus resonance amplitude measured at the output of the low-noise amplifier with 100× gain. The specified uncertainties of the points correspond to $\pm 1\sigma$. The solid line is the linear approximation of the experimental points.

frequency scanning, optimal model parameters are calculated, the microwave synthesizer frequency and the BWO power supply voltage are switched, and the attenuator position is adjusted, all of which result in unproductive time extensions. Starting from a certain value of τ_f, its further decrease has little effect on the recording time, as it is restricted by other processes. With allowance for all the above factors, $\tau_f = 45\ \mu$s was found to be the optimal value for the current spectrometer configuration. In this case, unproductive periods comprise approximately 30% of the entire time.

III. Specific Features of Obtaining the Gas Spectrum From Primary Data

A. Power Dependence of the Width of the Recorded Resonance Curve

In the longwave part of the working range, commercial waveguide detectors based on InP low-barrier planar diodes are used. As the current–voltage characteristics of diodes do not follow the quadratic law, the recorded resonance curve is slightly "flattened" leading to the systematic overestimation of its width, which grows with increasing radiation power. A weak dependence of the width on the resonance amplitude is observed even for a power less than 1 μW. Within the measurement error, the width depends linearly on the amplitude (see Fig. 4) as follows:

$$\Delta f = \Delta f_0 \cdot (1 + \beta \cdot A) \tag{3}$$

where Δf_0 is the unperturbed value of the width, A is the observed amplitude of the curve in volts, and β is the relative change in Δf when the amplitude changes by 1 V. The coefficient β is a characteristic of a detector that has no pronounced dependence on the resonance frequency and on the "unperturbed" value of its width. For the case depicted in Fig. 4, β is approximately 0.04 V^{-1}.

During the course of recording, the resonance amplitude at the output of the low-noise amplifier (100× gain) was set by an automatically controlled attenuator to be at a level of 60 mV, which corresponds to a detector response power of ∼0.5 μW. All the widths were normalized to the "unperturbed" values. The difference in the amplitude from the preset value at some points in the range due to insufficient source power was taken into account by the corresponding correction of the width Δf. It was shown that allowance for (3) permits increasing the signal-to-noise ratio in the experimental spectra [31].

Note that such calibration is needed only for the sake of convenience and the ease of working with commercial detectors in the mm range. No calibration is required when using a low-temperature bolometer, whose response varies in direct proportion to the power over a wide range, as a receiver. This allows the abovementioned attenuator adjustment to be avoided. The drawback of this variant is the inconvenience of working with liquid helium.

B. Impact of Standing Waves at Resonator Excitation on the Q-Factor

The resonator is connected to the external waveguide line; therefore, changes in the characteristics of the "resonator + external line" system lead to changes in the resonator characteristics. For example, the distance between the radiation source and the resonator expressed in wavelengths ("electrical" line length) changes as a result of the variation in the geometrical dimensions of the line (for example, with temperature variation), as well as due to changes in the radiation frequency during scanning. This leads to alterations in the interference pattern of the incident and reflected radiation in the line and, hence, to changes in the coupling coefficient between the resonator and the external line and, accordingly, the resonator Q-factor. The dependence of the resonator Q-factor on line length may be reduced by decreasing the coupling coefficient, which complicates registering the response; therefore, it has restrictions.

If the geometrical length of the line does not change during the experiment, this effect has no impact on the measurement result, as changes in the resonator Q-factor induced by interference are the same for recording the studied spectrum and for recording the baseline and are, thus, eliminated when the latter is subtracted.

Stabilization of the line temperature can significantly reduce this effect but does not eliminate it completely. To demonstrate the significance of the effect, the resonator response width is plotted in Fig. 5 as a function of the distance between the input horn antenna and the resonator axis. The width changes by approximately 4% due to parasitic interference. The regularity of this process allows a substantial reduction in the related systematic measurement error by averaging the absorption coefficient determined by (1) for several predetermined values of the distance between the radiation source and the resonator.

This effect is also observed in CRDS instruments ("etaloning," see, for example, [16], [32]), as the properties of the resonant system (resonator + coupled external line) do not depend on the registration method. The effect can be easily

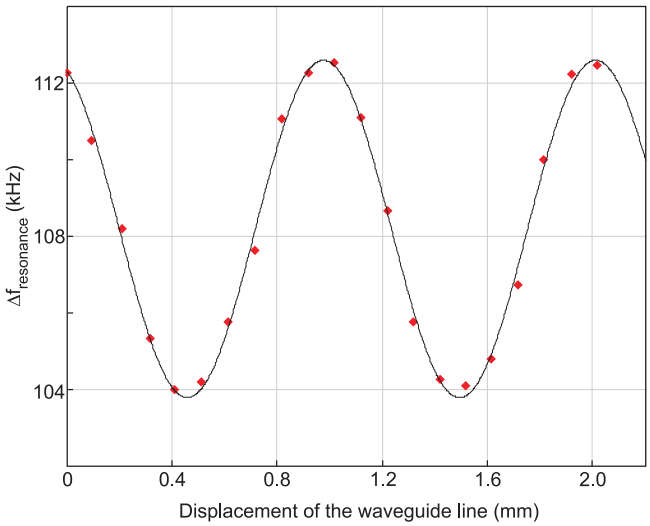

Fig. 5. Resonance curve half-width versus quasi-optical line displacement (see text). The points were obtained from the observed profiles (averaged over 100 scans), and the curve is the sine function fitted to the points. The period of the function is 1.036(18) mm (half-wavelength, $\lambda/2 = 1.024$ mm, $f = 146.405$ GHz). The coupling coefficient is 8×10^{-4}.

averaged in the IR region using the method of line length modulation by moving one of the auxiliary mirrors (e.g., [17]). However, dependence like that in Fig. 5 could be recorded accurately only with the use of our spectrometer.

C. Water Adsorption on Resonator Elements

The manifestations of this effect during the measurement of wet gas spectra are stronger when the closer the relative humidity is to 100% and the lower the temperature. It is difficult to separate the absorption in a gas and the absorption by water molecules adsorbed on the mirrors and coupling elements of the resonator; thus, a number of researchers in the past restricted themselves to stating the possibility of adsorption-related systematic error but did not find a way to quantify it. We solved this problem by using the method of optical path length variation, as described in detail in [22]. Here, we confine ourselves to a few remarks. First, as we have shown, the contribution of adsorbed molecules to the total absorption can be several times greater than the contribution of absorption in gas. Second, measures such as slight (by 5 °C) mirror heating to reduce the effect used, for example, by Liebe [12] do not ensure the desired result, as they are efficient for eliminating only "drop" condensation rather than adsorption. Substantial heating of the mirrors will lead, at least, to a change in the thermodynamic conditions in the cell. Third, it has been shown that the impact of the effect through the coupling element may be reduced significantly by using Teflon films (polytetrafluoroethylene), which are less hydrophobic than, for example, Mylar (polyethylene terephthalate) films [33].

The main idea of the method of optical path length variation in our spectrometer is the use of two resonators of different lengths with identical mirrors and coupling elements (see Fig. 2). If the lengths of the resonators and the losses in each of them are known, losses in gas and due to adsorbed water may be separated at the expense of a twofold reduction of the signal-to-noise ratio of the spectrum. In some cases (for example, when recording weak water dimer lines), such a reduction is unacceptable, so the choice of using two or only one "long" resonator depends on the specific study.

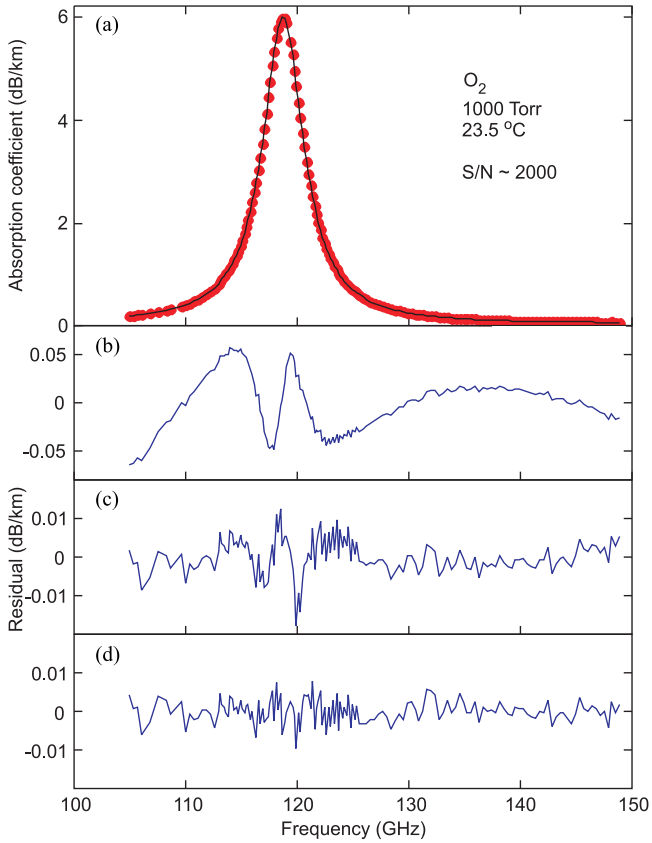

Fig. 6. (a) Experimental recording of the pure oxygen spectrum at 1000 torr and 23.5 °C. Residuals of model functions fitted to the experimental points based on different line shapes. (b) Van Vleck–Weisskopf profile. (c) Rosenkranz profile (LMVVW). (d) Quadratic speed-dependent line mixing Van Vleck–Weisskopf profile (qSDLMVVW) (see [31] for details).

IV. New Experimental Results

A. Diagnostic Oxygen Line Near 118 GHz

A single molecular oxygen line near 118 GHz was investigated in pure oxygen within the pressure interval of 250–1000 torr [31]. Analysis of the spectrum revealed, for the first time for this line, the influence of the speed dependence of the molecular collision cross section (the "wind" effect) and substantially improved the accuracy of the spectroscopic parameters of the line, such as collisional broadening, intensity, and mixing coefficients. An example of a line recording at a temperature of 23.5 °C and a pressure of 1000 torr is presented in Fig. 6. This corresponds to the averaging of four spectra obtained at different lengths of the quasi-optical line (see Section III-B). The signal-to-noise ratio is approximately 2000. The spectrometer sensitivity, defined as the absorption coefficient corresponding to one standard deviation of the background

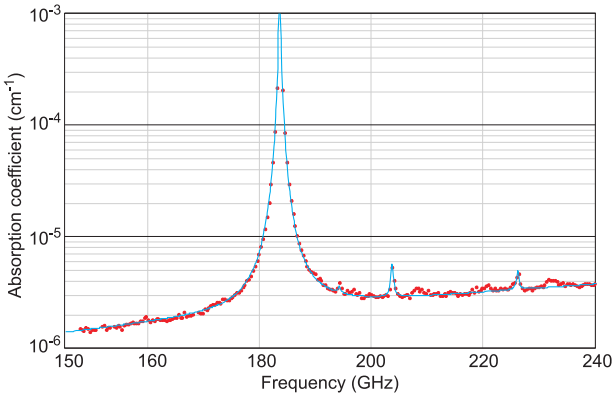

Fig. 7. Experimental spectrum of water vapor at $p = 12.3$ torr and room temperature (points). The solid line represents a model that includes water vapor resonance lines and a "smooth" continuum.

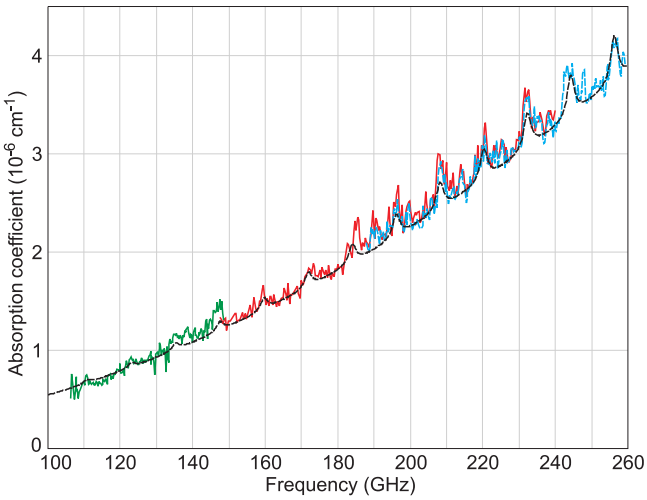

Fig. 8. Water vapor continuum absorption at room temperature. The thick green line is the spectrum from [26], the blue dotted line is the spectrum from [27], and the thin red line is the spectrum obtained in this paper. All spectra are normalized to a pressure of 12 torr. The thick black dotted line is a simplified model of the water dimer spectrum [27], [35].

noise, is 4×10^{-9} cm^{-1}. To increase the number of points for recording the line at pressures below the atmospheric pressure, measurements were made at several resonator lengths.

B. Resolved Rotational Spectrum of the Water Dimer

The unique capabilities of the spectrometer were demonstrated by studying the absorption spectrum of water vapor in the range of 150–240 GHz. In our previous work (see [34] and references therein), it was shown that this range is optimal for observing a series of water dimer peaks whose positions correspond to the rotation of the $(H_2O)_2$ molecule relative to the axis with maximum moment of inertia. We observed these series in the 105–150 [26] and 190–260 GHz bands [27].

Figs. 7 and 8 demonstrate the frequency and dynamic ranges over which the absorption coefficient can be measured by our spectrometer. The recording of the water vapor spectrum in the 150–240 GHz range, as well as the model function including the total contribution of water vapor lines (the diagnostic atmospheric line of water vapor near 183 GHz and a few less intense lines), and the "smooth" part of the continuum are shown in Fig. 7. The continuum spectrum presented in Fig. 8 clearly shows the dimeric series connecting the two previously observed sections of the dimer spectrum and allows obtaining a continuous sequence of 13 dimeric peaks. Fig. 8 demonstrates that even small inhomogeneities in the spectrum are not experimental noise. They recur in two recordings obtained with a four-year interval using resonators of different lengths, different waveguide lines, and different PLL systems. This leaves no doubt about the nature of the observed absorption. The obtained recording demonstrates the unique capabilities of the spectrometer—the dimer peaks are visible even against the background of the water line, the maximum absorption of which exceeds that of the dimer by more than two orders of magnitude.

V. Ultimate Sensitivity of Resonator Spectrometers

It is interesting to compare the physical sensitivity limits of various types of broadband microwave resonator spectrometers in which information on gas absorption is obtained from measurements of the quality factor of successive longitudinal modes of the Fabry–Perot resonator. Three main types of such spectrometers can be distinguished as follows.

1) A spectrometer with a free-running radiation source scanning a given range, for example, by changing the supply voltage of the source (see, for example, [15], [36]).
2) A Fourier spectrometer exciting the entire studied range by a "simple" or a "chirped" radiation pulse. Such spectrometers are currently used only for observation of molecular spectra (see, for example, [37], [38]), but they may also be used for observing a number of successive modes of the Fabry–Perot resonator.
3) A spectrometer using fast wideband precision control of radiation frequency, sequential scanning with continuous radiation phase of narrow areas around the resonance modes (see, Section II, [20], [22]), or, after accurate frequency switching to the center of each subsequent resonator mode, exciting this mode by a radiation pulse and receiving its "ringdown" response (CRDS mode).

These spectrometers contain prior information: Unlike the *a priori* unknown position of the spectral lines in the investigated molecular spectra, the frequencies of the resonator successive modes can be predetermined accurately. This avoids wasting time scanning empty, noninformative frequency regions between the resonator modes.

This prior information cannot be used in spectrometers of the first type for lack of a mechanism of precise control of the source frequency. It cannot be used in spectrometers of the second type either because of the simultaneous excitation of the entire studied range. Only in the third type of spectrometers accurate frequency control allows skipping noninformative spectral regions.

TABLE I
COMPARATIVE CHARACTERISTICS OF RESONATOR SPECTROMETERS OF DIFFERENT TYPES

Spectrometer type	Observation time of all resonance modes in one cycle	Receiver bandwidth	Number of cycles per t_1	Signal-to-noise ratio (one cycle)	Signal-to-noise ratio averaged over a number of cycles	Signal-to-noise ratio gain relative to that of a type-one spectrometer
1	$(\Delta F/\Delta f)n\tau$	Δf	1	$S/(\Delta f)^{1/2}$	$S/(\Delta f)^{1/2}$	1
2	τ	$\Delta\nu$	$(\Delta\nu/\Delta f)$	$S/(\Delta\nu)^{1/2}$	$(S/(\Delta\nu)^{1/2})(\Delta\nu/\Delta f)^{1/2}$	1
3	$n\tau$	Δf	$(\Delta F/\Delta f)$	$S/(\Delta f)^{1/2}$	$(S/(\Delta f)^{1/2})(\Delta F/\Delta f)^{1/2}$	$(\Delta F/\Delta f)^{1/2}$

As we are interested in ultimate sensitivity, for comparison, we will assume that all three types of spectrometers have the following features to be identical: 1) given frequency range to be studied; 2) receiver noise per unit band (for example, white thermal noise); 3) source power per spectral element (e.g., per mode response width); and 4) resonator Q-factors.

We introduce the following notations: $\Delta\nu$ is the width of the spectral range of interest; $n = \Delta\nu/\Delta F$ is the number of modes in the range, and $\Delta f = f/Q \sim 1/\tau$ is the resonance width, where τ is the decay time of free oscillations in the resonator.

The speed of frequency tuning in spectrometers of the first type is chosen from the condition of sufficient excitation of the resonator mode, i.e., it is defined by $\Delta f/\tau$. Then, the scanning time of the entire range with selected speed will be

$$t_1 = \Delta\nu/\left(\Delta f/\tau\right) = (\Delta F/\Delta f)\cdot n\tau. \tag{4}$$

The corresponding times required for one cycle observation of the entire spectrum for spectrometers of the second and third types are τ and $n\tau$, respectively. For calculation simplicity, we omit insignificant coefficients of the order of unity. For example, we take τ and Δf rather than $3\Delta f$ as the bandwidth in spectrometers of the first and third types and 3τ as the observation time for spectrometers of the second type.

We compare the signal-to-noise ratios of the three spectrometer types by averaging over the same time t_1, keeping in mind that under the abovementioned identical conditions, the amplitudes S of the signal responses from one mode will be identical for spectrometers of all the three types. When calculating the noise, we omit the identical multipliers kT. The corresponding parameters of the spectrometers obtained in this way are listed in Table I.

The performed comparative analysis shows that the spectrometers of the first and second types have identical ultimate sensitivity over time t_1. The gain obtained in spectrometers of the third type, compared to those of the first and second types, is directly proportional to the square root of the ratio of the FSR to the width of one resonator mode (finesse of the resonator). For real spectrometers, the gain can be more than one order of magnitude. For example, for the resonators used in [15] and [20], the gain would be approximately 20 and 50, respectively.

Practical implementation of this gain demands fast and precise (in some cases, continuous phase) frequency control of the radiation source throughout the studied range. At present, only our spectrometer can provide such control [21]. Note that source frequency control is currently being actively developed in the IR range as well (e.g., [32], [39], [40]). The main problems in the IR range are the difficulty of fast determination of the absolute value of radiation frequency, the impossibility of continuous precision scanning over the entire range of operating source frequencies, and in many cases, a rather broad radiation spectrum compared to the width of the resonator response. At the same time, the resonator Q-factor, which is higher in the IR range, enables an even greater gain in the ultimate sensitivity of the spectrometer. For example, the application of the above estimates to an IR resonator spectrometer [16], belonging to the first type according to the above classification, shows that its sensitivity can be increased approximately 600 fold.

Therefore, the main conclusions are as follows: 1) the use of *a priori* information allows a significant increase in the ultimate sensitivity of resonator spectrometers and 2) the extent to which ultimate sensitivity in spectrometers of this type may be increased will depend on the implementation of fast and precise (with a continuous radiation phase when operating in the frequency domain) control of the source frequency.

A system with fast and precise frequency control is becoming not only a technically but also a fundamentally important part of a spectrometer that determines the possibility of achieving ultimate sensitivity.

VI. CONCLUSION

The sensitivity and wide range of the IAP RAS resonator spectrometer achieved to date provide a successful solution to the broad scope of fundamental and applied problems of experimental spectroscopy, including the following.

1) Studies of the profile of wide atmospheric lines and subtle effects influencing this profile. For instance, manifestations of the "wind" effect for the oxygen line near 118 GHz and collisional coupling of the fine-structure oxygen lines have been thoroughly investigated, and as a result, parameters currently used in all mm and submm radiation propagation models have been obtained.
2) Refinement of the parameters of collisional broadening and shifting of the lines measured at low pressures by means of spectrometers of other types. The confidence in the obtained values of parameters increases significantly when the coefficients of line broadening and shifting measured at pressures differing by 3–4 orders of magnitude coincide within the statistical error (e.g., [25]). The pressure shifting of diagnostic lines was previously considered to be barely measurable and, hence, a negligible effect. Thanks to our work, this effect has been recognized

to be significant and has been included in propagation models.

3) Experimental verification of line intensities. No other method can compete with resonator spectroscopy in the accuracy of measuring this line parameter, as the measured absorption coefficient does not depend on the resonator length. According to the expert assessment by the creators of the spectroscopic database HITRAN, the uncertainty of the intensities of the mm and submm lines is 5%–10% for the majority of H_2O lines and 10%–20% for oxygen lines [41]. The indirect estimates based on the analysis of wide-range vibration-rotational spectra and high-precision measurements of individual lines in the IR range (see, e.g., [42], [43]) suggest that the accuracy of the present day calculations is actually higher about an order of magnitude. Nevertheless, the only coincidence of the results of calculating the intensities of many lines with the data from direct measurements by the resonator method gives the confidence that the error in modeling diagnostic lines corresponding to the use of calculated line intensities is unlikely to exceed 1%. Such experimental support improves the reliability and broadens the areas of application of modern global spectroscopic calculation methods.
4) Investigation of the spectral manifestation of gas nonideality, namely, continuum absorption, including spectra of dimers and free molecular pairs. Resonator spectroscopy has no real competitors in studying continuum in the mm and submm wavelength ranges. The application of other methods only confirm and supplement the obtained information. Resonator spectroscopy was used to investigate the dependence of the continuum on frequency, pressure, and temperature, which permitted the determination of the values of all the empirical coefficients needed for modeling the continuum in radiation propagation models. Resonator spectroscopy confirmed the hypothesis about the significant role of water vapor dimers in the formation of the atmospheric continuum, which had been actively discussed for more than half a century, and helped approach not only a full understanding of its nature but also the quantitative assessment of its principal components [44].

Sensitivity enhancement is highly desirable for further studies in all the research areas enumerated above. At present, several possible directions of spectrometer development that can lead to increased sensitivity should be noted.

The first is an increase in the signal-to-noise ratio during resonator response recording by using higher sensitivity receivers, such as cooled bolometers or superheterodyne receivers. In particular, this ensures the maximum possible reduction of the coupling coefficient and of the related effect of extraneous Q-factor modulating, discussed in Section III-B. A decrease in the coupling coefficient also means an increase in the resonator Q-factor, which is especially important in the shortwave part of the operating range.

Second, the resonator Q-factor can be improved by increasing its length. The sensitivity will increase in direct proportion to the distance between the mirrors. This method has natural limitations, as in the current version of the spectrometer, the resonator length is already 70 cm, which is close to the reasonable limit for conventional laboratory setups.

The third direction in spectrometer development is the reduction of remaining nonproductive time uses during the wide-range recording of spectra.

Finally, the maximum possible stability of the spectrometer waveguide line to mechanical (change in configuration, for example, due to pressure drops in the chamber) and thermodynamic action is demanded. Stable conditions will permit, if necessary, automatic accumulation of the signal for a longer time, thereby achieving higher sensitivity.

REFERENCES

[1] G. E. Becker and S. H. Autler, "Water vapor absorption of electromagnetic radiation in the centimeter wave-length range," *Phys. Rev.*, vol. 70, no. 5/6, pp. 300–307, Sep. 1946, doi: 10.1103/PhysRev.70.300.

[2] C. H. Townes and A. Schawlow, *Microwave Spectroscopy*. New York, NY, USA: Dover, 1975, pp. 435–441.

[3] Y. Beers, "Theory of the cavity microwave spectrometer and molecular frequency standard," *Rev. Sci. Instrum.*, vol. 30, no. 1, pp. 9–16, Jan. 1959, doi: 10.1063/1.1716366.

[4] E. P. Valkenburg and V. E. Derr, "A high-Q Fabry–Perot interferometer for water vapor absorption measurements in the 100 Gc/s to 300 Gc/s frequency range," *Proc. IEEE*, vol. 54, no 4, pp. 493–498, Apr. 1966, doi: 10.1109/PROC.1966.4763.

[5] W. S. Benedict, S. A. Clough, L. Frenkel, and T. E. Sullivan, "Microwave spectrum and rotational constants for the ground state of D_2O," *J. Chem. Phys.*, vol. 53, no. 7, pp. 2565–2570, Oct. 1970, doi: 10.1063/1.1674370.

[6] R. Pearson, T. Sullivan, and L. Frenkel, "Microwave spectrum and molecular parameters for $^{14}N_2\,^{16}O$," *J. Mol. Spectrosc.*, vol. 34, no. 3, pp. 440–449, Jun. 1970, doi: 10.1016/0022-2852(70)90025-1.

[7] J. Gilbert, "A microwave saturation spectrometer for the measurement of linewidth and absolute intensity," *Rev. Sci. Instrum.*, vol. 41, no. 7, pp. 1050–1065, Jul. 1970, doi: 10.1063/1.1684694.

[8] Yu. A. Dryagin and V. V. Parshin, "Concerning the possibility of measuring the absolute humidity of gases at low pressures," *Radiophys. Quantum Electron.*, vol. 16, no. 4, pp. 490–491, Apr. 1973, doi: 10.1007/BF01030902 (translated from Russian: Izvestiya Vysshikh Uchebnykh Zavedenii, Radiofizika, vol. 16, no. 4, pp. 638–640, April, 1973).

[9] L. Frenkel and D. Woods, "Microwave absorption by H_2O vapor and its mixtures with other gases between 100 and 300 Gc/s," *Proc. IEEE*, vol. 54, no. 4, pp. 498–505, Apr. 1966, doi: 10.1109/PROC.1966.4764

[10] L. Frenkel and D. Woods, "Microwave absorption in compressed CO_2," *J. Chem. Phys.*, vol. 44, no. 5, p. 2219, 1966, doi: 10.1063/1.1727018.

[11] H. J. Liebe, "Pressure-scanning mm-wave dispersion spectrometer," *Rev. Sci. Instrum.*, vol. 46, no. 7, pp. 817–825, Jul. 1975, doi: 10.1063/1.1134345.

[12] H. J. Liebe, "The atmospheric water vapor continuum below 300 GHz," *Int. J. Infrared Millim. Waves*, vol. 5, no. 2, pp. 207–227, Feb. 1984, doi: 10.1007/BF01417651.

[13] H. J. Liebe, P. W. Rosenkranz, and G. A. Hufford, "Atmospheric 60-GHz oxygen spectrum: New laboratory measurements and line parameters," *J. Quant. Spectrosc. Radiat. Transfer*, vol. 48, no. 5/6, pp. 629–643, Dec. 1992, doi: 10.1016/0022-4073(92)90127-P.

[14] A. Bauer, B. Duterage, and M. Godon, "Temperature dependence of water-vapor absorption in the wing of the 183 GHz line," *J. Quant. Spectrosc. Radiat. Transfer*, vol. 36, no. 4, pp. 307–318, Oct. 1986, doi: 10.1016/0022-4073(86)90054-3.

[15] A. I. Meshkov and F. C. De Lucia, "Broadband absolute absorption measurements of atmospheric continua with millimeter wave cavity ringdown spectroscopy," *Rev. Sci. Instrum.*, vol. 76, no. 8, Jul. 2005, Art. no. 083103, doi: 10.1063/1.1988027.

[16] S. Kassi and A. Campargue, "Cavity ring down spectroscopy with 5×10^{-13} cm^{-1} sensitivity," *J. Chem. Phys.*, vol. 137, no. 23, Dec. 2012, Art. no. 234201, doi: 10.1063/1.4769974.

[17] J. Burkart, D. Romanini, and S. Kassi, "Optical feedback frequency stabilized cavity ringdown spectroscopy," *Opt. Lett.*, vol. 39, no. 16, pp. 4695–4698, Aug. 2014, doi: 10.1364/OL.39.004695.

[18] D. A. Long, G.-W. Truong, R. D. van Zee, D. F. Plusquellic, and J. T. Hodges, "Frequency-agile, rapid scanning spectroscopy: Absorption sensitivity of 2×10^{-12} cm^{-1} Hz$^{-1/2}$ with a tunable diode laser," *Appl. Phys. B*, vol. 114, no. 4, pp. 489–495, Mar. 2014, doi: 10.1007/s00340-013-5548-5

[19] R. Gotti *et al.*, "Conjugating precision and acquisition time in a Doppler broadening regime by interleaved frequency-agile rapid-scanning cavity ring-down spectroscopy," *J. Chem. Phys.*, vol. 147, no. 13, Oct. 2017, Art. no. 134201, doi: 10.1063/1.4999056.

[20] A. F. Krupnov, M. Yu. Tretyakov, V. V. Parshin, V. N. Shanin, and S. E. Myasnikova, "Modern millimeter-wave resonator spectroscopy of broad lines," *J. Mol. Spectrosc.*, vol. 202, no. 1, pp. 107–115, Jul. 2000, doi: 10.1006/jmsp.2000.8104.

[21] M. Yu. Tretyakov, V. V. Parshin, M. A. Koshelev, A. P. Shkaev, and A. F. Krupnov, "Extension of the range of resonator scanning spectrometer into a submillimeter band and some perspectives of its further developments," *J. Mol. Spectrosc.*, vol. 238, no. 1, pp. 91–97, Jul. 2006, doi: 10.1016/j.jms.2006.04.016.

[22] M. Yu. Tretyakov *et al.*, "Resonator spectrometer for precise broadband investigations of atmospheric absorption in discrete lines and water vapor related continuum in millimeter wave range," *Rev. Sci. Instrum.*, vol. 80, no. 9, Sep. 2009, Art. no. 093106, doi: 10.1063/1.3204447.

[23] V. V. Parshin, M. Yu. Tretyakov, M. A. Koshelev, and E. A. Serov, "Modern resonator spectroscopy at submillimeter wavelengths," *IEEE Sens. J.*, vol. 13, no. 1, pp. 18–23, Jan. 2013, doi: 10.1109/JSEN.2012.2215315.

[24] V. V. Parshin *et al.*, "Cryogenic resonator complex," *Radiophys. Quantum Electron.*, vol. 56, no. 8/9, pp. 554–560, Jan. 2014, doi: 10.1007/s11141-014-9458-0 (Translated from Russian: Izvestiya Vysshikh Uchebnykh Zavedenii, Radiofizika, vol. 56, no. 8/9, pp. 614–621, Aug./Sep. 2013).

[25] A. F. Krupnov *et al.*, "Accurate broadband rotational BWO-based spectroscopy," *J. Mol. Spectrosc.*, vol. 280, pp. 110–118, Oct. 2012, doi: 10.1016/j.jms.2012.06.010.

[26] M. Yu. Tretyakov, E. A. Serov, M. A. Koshelev, V. V. Parshin, and A. F. Krupnov, "Water dimer rotationally resolved millimeter-wave spectrum observation at room temperature," *Phys. Rev. Lett.*, vol. 110, no. 9, Feb. 2013, Art. no. 093001, doi: 10.1103/PhysRevLett.110.093001.

[27] E. A. Serov, M. A. Koshelev, T. A. Odintsova, V. V. Parshin, and M. Yu. Tretyakov, "Rotationally resolved water dimer spectra in atmospheric air and pure water vapour in the 188–258 GHz range," *Phys. Chem. Chem. Phys.*, vol. 16, no. 47, pp. 26221–26233, Dec. 2014, doi: 10.1039/C4CP03252G.

[28] S. Nagarajan, C. F. Neese, and F. C. De Lucia, "Cavity-based medium resolution spectroscopy (CBMRS) in the THz: A bridge between high- and low-resolution techniques for sensor and spectroscopy applications," *IEEE Trans. THz Sci. Technol.*, vol. 7, no. 3, pp. 233–243, May 2017, doi: 10.1109/TTHZ.2017.2680841.

[29] M. Yu. Tretyakov, M. A. Koshelev, I. N. Vilkov, V. V. Parshin, and E. A. Serov, "Resonator spectroscopy of the atmosphere in the 350-500 GHz range," *J. Quant. Spectrosc. Radiat. Transfer*, vol. 114, pp. 109–121, Jan. 2013, doi: 10.1016/j.jqsrt.2012.08.019.

[30] R. I. Ovsyannikov and M. Yu. Tretyakov, "Determination of loss in a Fabry–Perot resonator from its response to exciting radiation with a fast-scanned frequency," *J. Commun. Technol. Electron.*, vol. 50, no. 12, pp. 1400–1408, 2005 (Translated from Russian: Radiotekhnika i Elektronika, vol. 50, no. 12, pp. 1509–1517, 2005).

[31] M. A. Koshelev *et al.*, "Accurate modeling of the diagnostic 118-GHz oxygen line for remote sensing of the atmosphere," *J. Quant. Spectrosc. Radiat. Transfer*, vol. 196, pp. 78–86, Jul. 2017, doi: 10.1016/j.jqsrt.2017.03.043.

[32] H. Lin, Z. D. Reed, V. T. Sironneau, and J. T. Hodges, "Cavity ring-down spectrometer for high-fidelity molecular absorption measurements," *J. Quant. Spectrosc. Radiat. Transfer*, vol. 161, pp. 11–20, Aug. 2015, doi: 10.1016/j.jqsrt.2015.03.026.

[33] M. A. Koshelev, E. A. Serov, V. V. Parshin, and M. Yu. Tretyakov, "Millimeter wave continuum absorption in moist nitrogen at temperatures 261–328 K," *J. Quant. Spectrosc. Radiat. Transfer*, vol. 112, no. 17, pp. 2704–2712, Nov. 2011, doi: 10.1016/j.jqsrt.2011.08.004.

[34] A. F. Krupnov, M. Yu. Tretyakov, and C. Leforestier, "Possibilities of observation of discrete spectrum of water dimer at equilibrium in millimeter-wave band," *J. Quant. Spectrosc. Radiat. Transfer*, vol. 110, no. 8, pp. 427–434, May 2009, doi: 10.1016/j.jqsrt.2009.01.022.

[35] T. A. Odintsova, M. Yu. Tretyakov, A. F. Krupnov, and C. Leforestier, "The water dimer millimeter-wave spectrum at ambient conditions: A simple model for practical applications," *J. Quant. Spectrosc. Radiat. Transfer*, vol. 140, pp. 75–80, Jun. 2014, doi: 10.1016/j.jqsrt.2014.02.016.

[36] I. R. Medvedev, "Submillimeter wave/THz technology and rotational spectroscopy of several molecules of astrophysical interest," Ph.D. dissertation, Ohio State Univ., Columbus, OH, USA, 2005.

[37] J. K. Ekkers and W. H. Flygare, "Pulsed microwave Fourier transform spectrometer," *Rev. Sci. Instrum.*, vol. 47, no. 4, pp. 448–454, Apr. 1976, doi: 10.1063/1.1134647.

[38] G. G. Brown *et al.*, "A broadband Fourier transform microwave spectrometer based on chirped pulse excitation," *Rev. Sci. Instrum.*, vol. 79, no. 5, May 2008, Art. no. 053103, doi: 10.1063/1.2919120.

[39] P. Čermák *et al.*, "CRDS with a VECSEL for broad-band high sensitivity spectroscopy in the 2.3 μm window," *Rev. Sci. Instrum.*, vol. 87, no. 8, Aug. 2016, Art. no. 083109, doi: 10.1063/1.4960769.

[40] R. Gotti, M. Prevedelli, S. Kassi, M. Marangoni, and D. Romanini, "Feed-forward coherent link from a comb to a diode laser: Application to widely tunable cavity ring-down spectroscopy," *J. Chem. Phys.*, vol. 148, no. 5, Feb. 2018, Art. no. 054202, doi: 10.1063/1.5018611.

[41] I. E. Gordon *et al.*, "The HITRAN2016 molecular spectroscopic database," *J. Quant. Spectrosc. Radiat. Transfer*, vol. 203, pp. 3–69, Dec. 2017, doi: 10.1016/j.jqsrt.2017.06.038.

[42] O. L. Polyansky *et al.*, "High-accuracy CO_2 line intensities determined from theory and experiment," *Phys. Rev. Lett.*, vol. 114, no. 24, Jun. 2015, Art. no. 243001, doi: 10.1103/PhysRevLett.114.243001.

[43] T. A. Odintsova *et al.*, "Highly accurate intensity factors of pure CO_2 lines near 2 μm," *J. Chem. Phys.*, vol. 146, no. 24, Jun. 2017, Art. no. 244309, doi: 10.1063/1.4989925.

[44] E. A. Serov, T. A. Odintsova, M. Yu. Tretyakov, and V. E. Semenov, "On the origin of the water vapor continuum absorption within rotational and fundamental vibrational bands," *J. Quant. Spectrosc. Radiat. Transfer*, vol. 193, pp. 1–12, May 2017, doi: 10.1016/j.jqsrt.2017.02.011.

Maksim A. Koshelev received the M.S. degree in radiophysics from the Radio Physical Faculty, Nizhny Novgorod State University, Nizhny Novgorod, Russia, in 2003, and the Ph.D. degree in physics from the Institute of Applied Physics, Russian Academy of Sciences, Nizhny Novgorod, in 2007.

Since 2000, he has been with the Microwave Spectroscopy Lab, Institute of Applied Physics, Russian Academy of Sciences, Nizhny Novgorod.

Igor I. Leonov received the combined B.S./M.S. degree in computer science from Gorky Polytechnic Institute, Nizhny Novgorod, Russia, in 1984.

Since 2014, he has been with the Institute of Applied Physics, Russian Academy of Sciences, Nizhny Novgorod, where he is currently a Senior Researcher.

Evgeny A. Serov received the M.S. degree in physics from the Advanced School of General and Applied Physics Faculty, Nizhny Novgorod State University, Nizhny Novgorod, Russia, in 2009, and the Ph.D. degree in physics from the Institute of Applied Physics, Russian Academy of Sciences, Nizhny Novgorod, in 2013.

Since 2005, he has been with the Microwave Diagnostics Lab, Institute of Applied Physics, Russian Academy of Sciences, Nizhny Novgorod.

Alena I. Chernova received the B.S. degree in computer science and applied math from Lobachevsky State University, Nizhny Novgorod, Russia, in 2013.

Since 2014, she has been a Software Developer Specialist with the Institute of Applied Physics, Russian Academy of Sciences, Nizhny Novgorod.

Aleksandr A. Balashov was born in Nizhny Novgorod, Russia, in 1995. He received the B.S. degree in physics from the Radio Physical Faculty, Nizhny Novgorod State University, Nizhny Novgorod, in 2017. He is currently working toward the degree at the Radiophysics Faculty, Nizhny Novgorod State University, Nizhny Novgorod.

Since 2016, he has been carrying out research work with the Microwave Spectroscopy Lab, Institute of Applied Physics, Russian Academy of Sciences, Nizhny Novgorod.

Grigoriy M. Bubnov (M'16) received the Master–Engineering degree in radio electronics from Nizhny Novgorod State Technical University, Nizhny Novgorod, Russia, in 2013.

Since 2013, he has been with the Institute of Applied Physics, Russian Academy of Sciences, Nizhny Novgorod, where he is currently a Junior Researcher. His scientific research interests include methods and techniques of mm/submm spectroscopy and atmospheric radiometry.

Aleksandr F. Andriyanov received the Master Engineering degree in radio engineering from the Gorky Polytechnic Institute, Nizhny Novgorod, Russia, in 1982.

Since 1977, he has been with the Institute of Applied Physics, Russian Academy of Sciences, Nizhny Novgorod, where he is a Leading Designer.

Aleksandr P. Shkaev received the Master Engineering degree in radio engineering from the Gorky Polytechnic Institute, Nizhny Novgorod, Russia, in 1970.

Since 1977, he has been with the Institute of Applied Physics, Russian Academy of Sciences, Nizhny Novgorod, where he is currently a Leading Designer.

Vladimir V. Parshin received the M.S. degree in radiophysics from Gorky State University, Nizhny Novgorod, Russia, in 1972.

Since 1977, he has been with the Institute of Applied Physics, Russian Academy of Sciences, Nizhny Novgorod, where he is currently a Senior Researcher. His research interests include quasi-optical and waveguide technique, technology of millimeter and submillimeter waves, and millimeter/submillimeter spectroscopy.

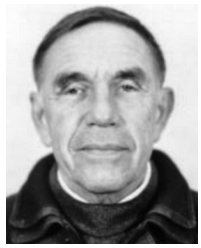

Andrei F. Krupnov was born on January 31, 1934. He received the M.S. degree in radiophysics and Ph.D. degree in physics from Gorky State University, Nizhny Novgorod, Russia, in 1957 and 1965, respectively, and the Dr.Sc. degree in physics from Lebedev Physical Institute, Moscow, Russia, in 1975.

He was the Head of the Microwave Spectroscopy Department (1977–2005). From 1976 to 2009, he was a member of the Editorial Board of the *Journal of Molecular Spectroscopy*. He is currently a General Research Associate with the Institute of Applied Physics, Russian Academy of Sciences, Nizhny Novgorod.

Prof. Krupnov was a recipient of the State Prize of the USSR in 1980, for development of submillimeter-wave spectroscopy based on backward wave oscillators.

Mikhail Yu. Tretyakov received the M.S. degree in radiophysics from Gorky State University, Nizhny Novgorod, Russia, in 1980, and the Dr.Sc. degree in physics from the Institute of Applied Physics, Russian Academy of Sciences, Nizhny Novgorod, in 2017.

Since 1980, he has been with the Institute of Applied Physics, Russian Academy of Sciences, Nizhny Novgorod, where he is currently the Head of the Laboratory of Microwave Spectroscopy. Since 2015, he has been a member of the Editorial Board of the *Journal of Molecular Spectroscopy*.